Direct semiclassical simulation of photochemical processes with semiempirical wave functions

G. Granucci, M. Persico, and A. Toniolo

Citation: J. Chem. Phys. **114**, 10608 (2001); doi: 10.1063/1.1376633
View online: http://dx.doi.org/10.1063/1.1376633
View Table of Contents: http://jcp.aip.org/resource/1/JCPSA6/v114/i24
Published by the AIP Publishing LLC.

Direct semiclassical simulation of photochemical processes with semiempirical wave functions

G. Granucci and M. Persico
Dipartimento di Chimica e Chimica Industriale, Università di Pisa, via Risorgimento 35, I-56126 Pisa, Italy

A. Toniolo
Dipartimento di Chimica Fisica ed Elettrochimica, Università di Milano, via Golgi 19, I-20133 Milano, Italy

(Received 26 January 2001; accepted 11 April 2001)

We describe a new method for the simulation of excited state dynamics, based on classical trajectories and surface hopping, with direct semiempirical calculation of the electronic wave functions and potential energy surfaces (DTSH method). Semiempirical self-consistent-field molecular orbitals (SCF MO's) are computed with geometry-dependent occupation numbers, in order to ensure correct homolytic dissociation, fragment orbital degeneracy, and partial optimization of the lowest virtuals. Electronic wave functions are of the MO active space configuration interaction (CI) type, for which analytic energy gradients have been implemented. The time-dependent electronic wave function is propagated by means of a local diabatization algorithm which is inherently stable also in the case of surface crossings. The method is tested for the problem of excited ethylene nonadiabatic dynamics, and the results are compared with recent quantum mechanical calculations. © *2001 American Institute of Physics.*
[DOI: 10.1063/1.1376633]

I. INTRODUCTION

The computational simulation of photochemical reactions is a very powerful complement to experiment. It allows to interpret measurements in a mechanistic way and to investigate details that would go undetected in many refined experiments; it has also a predictive ability and may stimulate new laboratory research. The standard simulation procedure, based on the Born–Oppenheimer scheme, goes through three steps. First, one calculates adiabatic potential energy surfaces (PES), nonadiabatic or magnetic couplings and other electronic matrix elements which may be needed. All these quantities are functions of the nuclear coordinates, so the second step is to represent PESs and couplings analytically by some kind of interpolation or fitting technique. Third, one can run excited state dynamics, either by quantum-mechanical or by (semi)classical methods: the focus here may be on the nuclear motion only,[1,2] or on vibronic transitions of quasi-bound states,[3] but most of the time electronic and nuclear dynamics are strongly coupled[4–9] (the quoted papers are but a few examples of a vast literature, more can be found in their references).

When conical intersections or other near degeneracy regions are present, the adiabatic representation of the electronic states is usually supplemented with convenient alternatives, based on (quasi-)diabatic states[10,11] or valence-bond (VB) structures, as first suggested by Warshel.[12,13] The minimal purpose of these tools is to facilitate the fitting of the PES and the calculation of dynamical couplings; however, such procedures actually replace the analytical representation of the PES and couplings by a very simple quantum-mechanical calculation based on a model electronic Hamiltonian,[8] to be performed at need during the simulation of the dynamical process. Empirical VB models, in particular, are fairly transferable, so their status is above that of mere fitting tools, and dynamical simulations based on such schemes are rightly qualified as ''direct'' or ''on-the-fly,'' in that the three steps of electronic calculation, fitting, and dynamics, do collapse into one.[4,7] The empirical VB parameters are adjusted so as to reproduce *ab initio* or experimental results: in fact, a previous knowledge of some sections of the *ab initio* PES is usually required. Direct dynamics based on *ab initio* methods, without the intermediation of model Hamiltonians, has been run first for the ground state, from the pioneering work by Leforestier[14] to the success of Car–Parrinello method.[15] Direct *ab initio* simulations of photochemistry are a recent development.[16–18] As excited state calculations are more demanding in terms of computer resources, *ab initio* direct dynamics in this field may face severe limitations.

The aim of the present work is to develop a method for direct nonadiabatic dynamics, based on semiempirical molecular orbital–configuration integration (MO–CI) wave functions and energies. Semiempirical models for excited states[19–22] are now validated for many classes of compounds. With respect to *ab initio* methods, they are obviously much faster, therefore more suitable for direct dynamics. With proper parametrization, they can reproduce essential portions of the excited PES better than widely employed but not very refined *ab initio* techniques, such as complete active space SCF (CASSCF). In comparison with empirical VB models, they offer a wider range of applicability, in that parametrizations are already available for scores of elements. However, some adjustments are necessary at least when one is interested in photodissociations, because most semiempirical methods rely upon closed shell SCF: the improvements we

have introduced, already presented in a previous paper,[23] are shortly described in Sec. II.

Direct methods are most naturally conjugated with classical nuclear dynamics; in fact, each time step in a nuclear trajectory corresponds to one molecular geometry and calls for one electronic calculation, while the nonlocal character of quantum mechanics in principle prevents such a simple approach. Therefore we have set up a semiclassical method, where the nuclear motion is treated classically and the electrons are represented by a time-dependent wave function; surface hopping, in Tully's ''fewest switches'' version,[24,25] provides the link between the two physical descriptions. The surface hopping model has been compared with rigorous quantum-mechanical calculations in model as well as real systems, and its results have been found satisfactory except probably in limiting cases.[9,26–29] We shall denote the method presented here by the acronym DTSH (direct trajectories with surface hopping). In spite of the basic problem of delocalization, a more rigorous fully quantal approach to direct dynamics can be envisaged, as shown by Martinez and co-workers:[17] their *ab initio* ''multiple spawning'' method (AIMS) is computationally efficient as far as the nuclear wave packets do not spread or split too much. Our reformulation of semiempirical MO–CI techniques may find application also in that context.

In Sec. II we describe the direct semiempirical approximation of electronic energies and wave functions and the integration of classical trajectories, i.e., all what is needed to run one-state dynamics. In Sec. III we discuss the solution of the time-dependent Schrödinger equation for the electrons and the modelling of nonadiabatic transitions. Finally, in Sec. IV we test the method on a well known photochemical process, namely geometrical and electronic relaxation of excited ethylene.

II. TRAJECTORIES AND ELECTRONIC CALCULATIONS

We consider a system with nuclear degrees of freedom **Q** and electronic degrees of freedom **q**. The nuclei are treated as classical particles while the electrons are quantum mechanical. The potential energy surfaces $E_K(\mathbf{Q})$ and their gradients, which govern the nuclear motion, are obtained on the fly, by solving at each integration step the time independent Schrödinger equation for electrons at fixed nuclei, i.e., by finding approximate eigenvalues and eigenfunctions of the electronic Hamiltonian $\hat{\mathcal{H}}_{\mathrm{el}}$.

The method for the calculation of the electronic states within the DTSH scheme should fulfill the following requirements: (a) to yield approximate solutions for the ground and several excited states on an equal footing; (b) to behave correctly for all the nuclear configurations explored during a trajectory, i.e., to deal with bond breaking processes, state degeneracies, etc.; (c) to be computationally viable. With *ab initio* methods the fulfillment of conditions (a) and (b) results in too expensive computations, except maybe for very small molecular systems. We have therefore considered semiempirical methods, using a variant[23] recently implemented by us in a development version of the MOPAC[21] package: the electronic wave functions are of the configuration interaction (CI) type, with molecular orbitals (MO) obtained in a single determinant SCF calculation with fractional, and possibly variable (''floating''), occupation numbers.

An SCF with fractional (floating) occupation is formally of the closed shell type, but in the definition of the density matrix $\boldsymbol{\rho}$ one introduces occupation numbers N_k, which may differ from 0 or 2:

$$\rho_{ij}=\sum_k N_k C_{ik} C_{jk}, \tag{1}$$

where C_{ik} is the kth MO coefficient for the ith basis function.[30,31] In our procedure the orbitals are partitioned into inactive, active and virtuals; only the active MO's have fractional occupations, which may be either arbitrarily fixed, or floating. In the latter instance, the N_k values are self-consistently determined according to the orbital energies ε_k:

$$N_k=\frac{\sqrt{2}}{\sqrt{\pi}w}\int_{-\infty}^{\varepsilon_F}\exp\left[-\frac{(\varepsilon-\varepsilon_k)^2}{2w^2}\right]d\varepsilon. \tag{2}$$

The Fermi level ε_F is in turn adjusted so that $\Sigma_k N_k$ is the total number of electrons. In Eq. (2), w is an arbitrarily chosen orbital energy width parameter, which determines the spread of electronic populations below and above the Fermi level. In the truncation of the CI space we only consider excitations within the active MO's; usually, a CAS–CI is done (full CI within the active orbital space). In order to run trajectories and also geometry optimizations, we have implemented for the first time analytical derivatives of the CI energies with floating occupation MO's with respect to nuclear coordinates.[23]

Fractional occupation ($N_k=1$ for HOMO and LUMO) is needed for a correct treatment of homolytic bond breaking, and also in the analogous situation of double bond twisting. When the dissociation fragments include atoms or diatomics, one has the additional problem of orbital degeneracy, which often requires a further partition of electron charge among the valence orbitals. If more than one dissociation channel is envisaged, in general the charge neutrality and degeneracy requirements cannot be satisfied by a single occupation pattern: one must then resort to floating occupation, automatically adjusting to the molecular geometry. Because some orbitals above the Fermi level are partially filled, they are optimized to a certain extent, thus improving the description of excited states. This is particularly important when uncompletely filled shells are dealt with, as in the case of transition metal compounds. In *ab initio* calculations, all these problems are usually taken care of by means of state-average CASSCF calculations, possibly followed by a larger CI. Apart from its inherent drawbacks, such as root switching along with geometrical variations, CASSCF is too expensive to be employed in conjunction with semiempirical techniques. The floating occupation SCF + CI procedure can be regarded as a computationally effective substitute for CASSCF.

Many semiempirical parametrizations were optimized within the closed shell SCF approximation for the ground state; the excited states, when taken into account, were often

represented by a CI of singly excited determinants. Therefore, the standard parameters may not be optimal for a CAS–CI with floating occupation MO's. In fact, the electron correlation would be taken into account twice, first at the level of the original parametrization, and then partly by the CI procedure (although a small CI in a minimal basis set does not allow for dynamical correlation effects). Therefore, a modification of the semiempirical parameters may be necessary. In general it is advisable to define a minimal MO active space for the CAS–CI calculation, sufficient to represent all the electronic states along the reaction pathways of interest. The fractional MO occupations are often imposed by formal neutrality and MO degeneracy requirements for the dissociating fragments; if the floating occupation SCF is used, the MO energy width w can be set to a reasonable value (usually between 0.1 and 0.5 a.u.), chosen in order to achieve easy convergence of the SCF process at all geometries;[32] in practice, w can be used as an adjustable parameter, to improve the quality of the computed PES. Once defined the SCF and CI procedures to be adopted, in most cases it will be important to recalibrate some or all of the semiempirical parameters, with the goal of reproducing experimental or *ab initio* results for the particular system under study. This can be done by minimizing a target function of the parameters, defined as a weighted sum of square deviations (semiempirical versus *ab initio* or experimental) for a set of molecular observables: electronic transition energies, barriers, dissociation energies, bond lengths, and angles, etc.; since no analytic gradients with respect to the semiempirical parameters are available for these quantities, and the target function has likely multiple minima, suitable optimization procedures are the simplex method or simulated annealing.[33] Our (so far rather limited) experience shows that moderate alterations of standard MINDO/3,[34] AM1[35] or MNDO/d[36] parameters yield PES of a good quality.[37]

The time evolution of the nuclei, i.e., of the classical degrees of freedom $\mathbf{Q}$, is performed by integrating Newton's equations, the potential being a given adiabatic surface $E_K(\mathbf{Q})$. Using a Verlet-type numerical integration[38] we obtain

$$Q_\alpha(t+\Delta t)=Q_\alpha(t)+\dot{Q}_\alpha(t)\Delta t + \frac{\Delta t^2}{m_\alpha}\left[\frac{2}{3}F_\alpha(t)-\frac{1}{6}F_\alpha(t-\Delta t)\right]+O(\Delta t^4), \tag{3}$$

$$\dot{Q}_\alpha(t+\Delta t)=\dot{Q}_\alpha(t)+\frac{\Delta t}{m_\alpha}\left[\frac{5}{6}F_\alpha(t)+\frac{1}{3}F_\alpha(t+\Delta t) - \frac{1}{6}F_\alpha(t-\Delta t)\right]+O(\Delta t^4), \tag{4}$$

where α labels the nuclear coordinates, m_α are the nuclear masses, and $F_\alpha=-\partial E_K/\partial Q_\alpha$. At each integration time step, the $Q_\alpha(t+\Delta t)$ are evaluated by Eq. (3), the gradients $F_\alpha(t+\Delta t)$ are calculated and then the velocities $\dot{Q}_\alpha(t+\Delta t)$ can be obtained using Eq. (4).

Swarms of trajectories are usually run, with randomly selected initial conditions. The statistical analysis of results then allows to extract several observables, such as product quantum yields, final electronic states, fragment velocity distributions, and anisotropies. In many cases the initial conditions should be sampled from a Boltzmann distribution of nuclear coordinates and momenta in the ground electronic state, which can be easily reproduced by Langevin dynamics, i.e., letting the molecular system do a Brownian motion until equilibration. We have therefore implemented the integration of Langevin's equation, following van Gunsteren and Berendsen:[39]

$$\ddot{Q}_\alpha=-\gamma_\alpha V_\alpha+\frac{F_\alpha(t)}{m_\alpha}+X_\alpha(t), \tag{5}$$

where γ_α are the friction coefficients[40] and $X_\alpha(t)$ is a Gaussian random white noise. Note that, in presence of a dissipative term in the force acting on the nuclei, Eq. (4) must be sligthly modified; in particular, defining $G_\alpha=F_\alpha-m_\alpha\gamma_\alpha\dot{Q}_\alpha$ one obtains

$$\dot{Q}_\alpha(t+\Delta t)=\frac{3}{3+\gamma_\alpha\Delta t}\left\{\dot{Q}_\alpha(t)+\frac{\Delta t}{m_\alpha}\left[\frac{5}{6}G_\alpha(t) + \frac{1}{3}F_\alpha(t+\Delta t)-\frac{1}{6}G_\alpha(t-\Delta t)\right]\right\}+O(\Delta t^4). \tag{6}$$

Note that Langevin's dynamics can also be taken as a simple model of solute–solvent energy transfer, in order to simulate condensed phase photochemistry.[40]

III. TIME EVOLUTION OF THE ELECTRONIC WAVE FUNCTION

The time-dependent electronic wave function can be expanded in the adiabatic basis:

$$|\Psi(t)\rangle=\sum_K A_K(t)|\psi_K(t)\rangle. \tag{7}$$

The time evolution of the A_K coefficients is dictated by the Schrödinger equation,

$$i\frac{d}{dt}|\Psi(t)\rangle=\hat{\mathcal{H}}_{el}(t)|\Psi(t)\rangle \tag{8}$$

(atomic units are used, $\hbar=1$). The electronic Hamiltonian $\hat{\mathcal{H}}_{\mathrm{el}}$ and its eigenfunctions ψ_K depend on time through the nuclear coordinates. Any approximate solution of this equation, based on the adiabatic representation (7) and on a finite order expansion in powers of t, is liable to inaccuracy in case of weakly avoided curve crossings, or in close proximity of conical intersections: in fact, quasidegeneracy may entail sudden variations of the eigenfunctions $\psi_K(t)$ and of the coefficients $A_K(t)$, divergencies in the nonadiabatic matrix elements, and nonlinear behaviors of the eigenvalues E_K along the trajectory (cusps or near cusps). In view of the strong interest of quasidegenerate situations in the simulation of nonadiabatic dynamics, we want our algorithm to be inherently stable also in such cases. To this aim, we shall resort to a ''locally diabatic'' representation, i.e., to a set of electronic states which are specifically diabatic along the nuclear trajectory under consideration. For the general concept of

diabatic states, we refer to recent reviews.[10,11] The idea of relating the adiabatic to diabatic transformation to a given path in the coordinate space can be traced back to the work of Baer,[41] Gadéa and Pélissier,[42] and Petsalakis *et al.*[43]

Usually one can restrict the dynamical treatment to the first N electronic states $\{\psi\}$, for instance on the basis of energetic considerations: the $\{\psi\}$ will span the ''internal'' subspace, while all the ψ_K with $K>N$ belong to the ''external'' subspace. By definition, the diabatic basis also spans the internal subspace and is connected with the adiabatic one by a unitary transformation $\mathbf{T}$,

$$\{\boldsymbol{\eta}\}\mathbf{T}(t)=\{\boldsymbol{\psi}\}. \tag{9}$$

If $\mathbf{H}$ is the Hamiltonian in the diabatic basis ($H_{IJ}=\langle\eta_I|\hat{\mathcal{H}}_{\rm el}|\eta_J\rangle$) and $\mathbf{E}$ the diagonal matrix of the electronic energies, we have

$$\mathbf{HT}=\mathbf{TE}. \tag{10}$$

The diabatic expansion of the time-dependent wave function is

$$|\Psi(t)\rangle=\sum_I^N D_I(t)|\eta_I(t)\rangle \tag{11}$$

with

$$\mathbf{D}=\mathbf{TA}. \tag{12}$$

For a sake of simplicity, let us set the time at the beginning of a generic trajectory step as $t=0$; then we have $t=\Delta t$ at the end of the step. We redefine the locally diabatic basis at each step, as follows. At the beginning of the step, we choose $T(0)$ to be the identity matrix, so $\eta_I\equiv\psi_I$. For a generic electronic basis $\{\boldsymbol{\eta}\}$, the expansion coefficients would obey the equations

$$\frac{dD_I}{dt}=-\sum_J^N D_J(t)\sum_\alpha\left[\dot{Q}_\alpha\left\langle\eta_I\left|\frac{\partial}{\partial Q_\alpha}\right|\eta_J\right\rangle+iH_{IJ}\right]$$
$$=-\sum_J^N D_J(t)\sum_\alpha\left[\left\langle\eta_I\left|\frac{d}{dt}\right|\eta_J\right\rangle+iH_{IJ}\right]. \tag{13}$$

We choose the diabatic states so as to eliminate the dynamic couplings: $\langle\eta_I|d/dt|\eta_J\rangle=0$ for $I,J\leqslant N$. Notice however that the couplings only vanish along the advancement coordinate identified by the velocity vector $\dot{\mathbf{Q}}$: in this sense the $\{\boldsymbol{\eta}\}$ are ''locally'' diabatic for the given trajectory. Equation (13) then reduces to

$$\frac{d\mathbf{D}}{dt}=-i\mathbf{HD}. \tag{14}$$

The $\mathbf{T}$ matrix at time Δt, whence the $\{\boldsymbol{\eta}\}$ functions and the Hamiltonian $\mathbf{H}$, is related to the overlap between adiabatic functions at the beginning and at the end of the time step:

$$S_{KL}=\langle\psi_K(0)|\psi_L(\Delta t)\rangle=\sum_I^N\langle\eta_K(0)|\eta_I(\Delta t)\rangle T_{IL}(\Delta t) \tag{15}$$

(see Appendix A for the calculation of the S_{KL} overlaps). In fact, we show in Appendix B that $\mathbf{T}(\Delta t)$ can be approximated by Löwdin's orthogonalization of the columns of $\mathbf{S}$. From $\mathbf{T}(\Delta t)$ one gets $\mathbf{H}(\Delta t)$ and the propagation operator in the diabatic basis, $\exp(-i\mathbf{Z}\Delta t)$, with $\mathbf{Z}=[\mathbf{E}(0)+\mathbf{H}(\Delta t)]/2$. Finally, the adiabatic expansion coefficients $\mathbf{A}(\Delta t)$ are computed through the inverse of Eq. (12):

$$\mathbf{A}(\Delta t)=\mathbf{T}^t e^{-i\mathbf{Z}\Delta t}\mathbf{A}(0)=\mathbf{UA}(0). \tag{16}$$

The unitarity of the transformation $\mathbf{U}=\mathbf{T}^t e^{-i\mathbf{Z}\Delta t}$ enforces the exact conservation of the norm of the time-dependent wave function. For the propagation of the electronic wave function one does not need more that the adiabatic to diabatic transformation within a time step. However, the overall transformation along a given trajectory, from the beginning to any time, can be computed as the product of all the $\mathbf{T}(\Delta t)$ matrices.

A surface hopping may take place at each step, according to Tully's fewest switches strategy.[24,25] The hopping probability from state ψ_K to state ψ_L, at the end of a time step Δt, is

$$P_{K\to L}=\frac{B_{KL}}{|A_K(0)|^2}, \tag{17}$$

where B_{KL} is the contribution of state ψ_L to the increment of the population $|A_K|^2$ of state ψ_K; if $B_{KL}<0$, then $P_{K\to L}$ vanishes. Within our algorithm, the change of $|A_K|^2$ in a time step is

$$|A_K(\Delta t)|^2-|A_K(0)|^2=\sum_{L,L'}U_{KL}U^*_{KL'}A_L(0)A^*_{L'}(0)$$
$$-|A_K(0)|^2. \tag{18}$$

This expression can be recast as $-\Sigma_{L(\neq K)}B_{KL}$ if

$$B_{KL}=-\Re[U_{KL}A_L(0)A^*_K(\Delta t)]$$
$$\times\frac{|A_K(\Delta t)|^2-|A_K(0)|^2}{|A_K(\Delta t)|^2-\Re[U_{KK}A_K(0)A^*_K(\Delta t)]} \tag{19}$$

for $K\neq L$ ($B_{KK}=0$). Notice that, to first order in Δt, with $U_{KL}=\delta_{KL}+iR_{KL}\Delta t$, one gets $B_{KL}=2\Delta t\Im[A^*_K(0)R_{KL}A_L(0)]=-B_{LK}$. In the preceding expressions, $\Re$ and $\Im$ mean real and imaginary part of complex quantities.

Average state populations $P_K(t)$ are defined over many trajectories, from the probabilities $|A_K|^2$. The actual distributions $\Pi_K(t)$ of the trajectories on the adiabatic PES should coincide with the computed $P_K(t)$ populations, an ideal requirement that is satisfied only approximately by most surface hopping algorithms (see for instance Fang and Hammes-Schiffer[44] and references therein).

IV. SIMULATION OF ETHYLENE NONADIABATIC DYNAMICS

We have tested the DTSH method on a well-known example, the geometrical and electronic relaxation of the S_1 state of ethylene. After some pioneering work done about 20 years ago,[45,46] the process has been recently studied theoretically by the multiple spawning (AIMS) method[17,47] and experimentally by ultrafast pump-probe spectroscopy.[48,49]

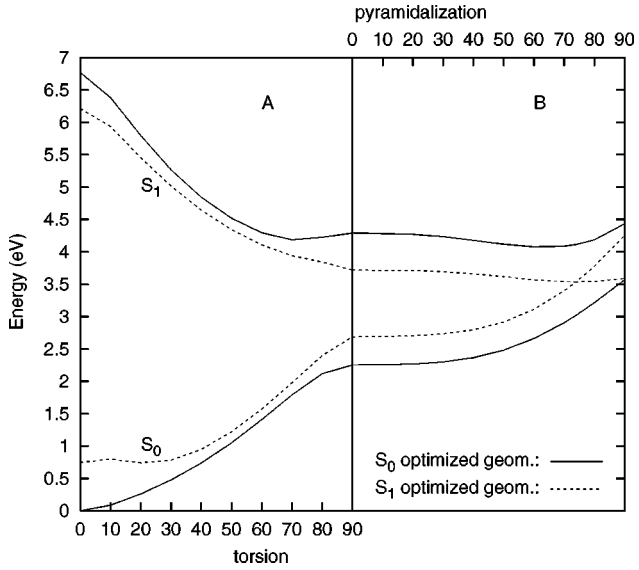

FIG. 1. Potential energy curves for the two lowest singlets of ethylene, MINDO/3 CAS–CI (see text). Left panel (A) torsion only, no pyramidalization. Right panel (B) torsion angle $\theta=90°$, pyramidalization of one carbon atom. Full curves, bond lengths and bond angles optimized in the S_0 PES (with given torsion and pyramidalization angles); dashed curves, bond lengths and angles optimized in the S_1 PES.

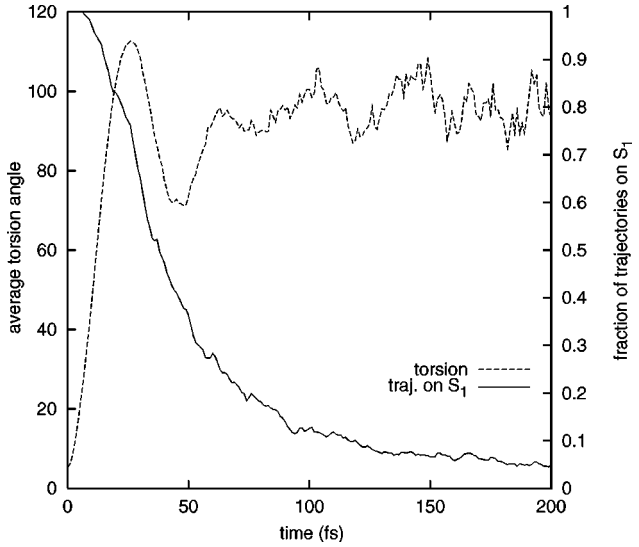

FIG. 2. Average torsion angle $\langle\theta\rangle$ and fraction of trajectories in S_1, as functions of time.

According to the best *ab initio* calculations,[17,50,51] the vertical excitation energy is about 8 eV while in the twisted D_{2d} geometry the S_1 state lies 5.5 eV above the planar ground state.[52] The pyramidalization of one carbon atom further lowers the S_1 energy by at least 0.5 eV. Around 80° of pyramidalization, the S_0 and S_1 PESs intersect each other. The resulting conical intersection is held responsible for the very fast decay of S_1. In this preliminary work, we have employed the standard MINDO/3 parameters,[34] floating occupation SCF with $w=0.2$ a.u., and an active space of two electrons in two orbitals (π and π^*). This yields the potential energy curves shown in Fig. 1. The excited state energy is altogether slightly underestimated, but the qualitative features of the PES are quite well reproduced, including the S_0-S_1 conical intersection.

Initial conditions for 750 trajectories were selected so as to reproduce the normal mode quantum mechanical distribution of coordinates and momenta. Figure 2 shows the population of S_1 as a function of time, along with the average torsion angle $\langle\theta\rangle$, where $\theta=(\angle H_1C_1C_2H_3+H_1C_1C_2H_4+H_2C_1C_2H_3+H_2C_1C_2H_4-360°)/4$; the definition of θ is such that planar ethylene has $\theta=0$ and a symmetric decrease of both CCH angles for one methylene moiety (pyramidalization), does not affect θ. Because each trajectory is stopped when its potential energy goes below 2.5 eV on the ground state PES, the number of trajectories which concur to define the average $\langle\theta\rangle$ rapidly decreases in time, and the plot becomes more and more ''noisy.'' However, one can see that most trajectories do not go beyond one oscillation in the S_1 PES before they hop down to S_0. Both the torsional motion and the internal conversion are somewhat faster than computed with AIMS:[17] the AIMS lifetime of S_1 is about 180 fs, while we get about 50 fs. Superficially, one might say that the latter value is in better agreement with the experimental findings than the former: in fact, decay times of 20 to 30 fs were measured by two different groups[48,49] by means of probe pulse ionization. However, probably ionization can take place only in the proximity of the Franck–Condon region, therefore the experiments only detect the initial part of the geometrical relaxation dynamics on the S_1 PES, rather than the S_1-S_0 decay.[17] Further simulations are planned to model in a realistic way the pump–probe experiments.

In Fig. 3 we show the distribution of bond and pyramidalization angles at the time of the first surface hopping. Notice that most trajectories undergo just one hopping event, because their downward motion on the ground state PES rapidly increases the S_0-S_1 energy gap, thus making further transitions quite unlikely. In the upper panel we show the distribution of the smallest CCH angle ($\angle C_2C_1H_1$), and of the other bond angle for the same methylene moiety ($\angle C_2C_1H_2$). In the middle panel we show the two angles of the other methylene ($\angle C_1C_2H_3$ and $\angle C_1C_2H_4$). Most transitions take place at distorted geometries, where one of the four angles is much smaller that the other three, and the corresponding hydrogen atom is in a bridging position between C_1 and C_2. Also the two pyramidalization angles (each defined as the angle between the bisector of one HCH and the CC axis) have different distributions: one carbon atom tends to be more pyramidalized than the other one (see lower panel of Fig. 3). These findings are in agreement with the AIMS results[17] and previous *ab initio* explorations of the PES.[50]

In Fig. 4 we show the energy difference between S_1 and S_0 at the time of the first surface hopping. Of course, the hopping events concentrate at geometries where the energy gap is small (<0.5 eV), but a significant fraction of them occur between 0.5 and 2 eV. Although really accurate comparisons are not possible, according to the AIMS treatment the nonadiabatic transitions are more strictly confined to the surface crossing region.[47] This discrepancy may result from differences in the treatment of the nonadiabatic dynamics: in DTSH, approximations are inherent to the underlying theory;

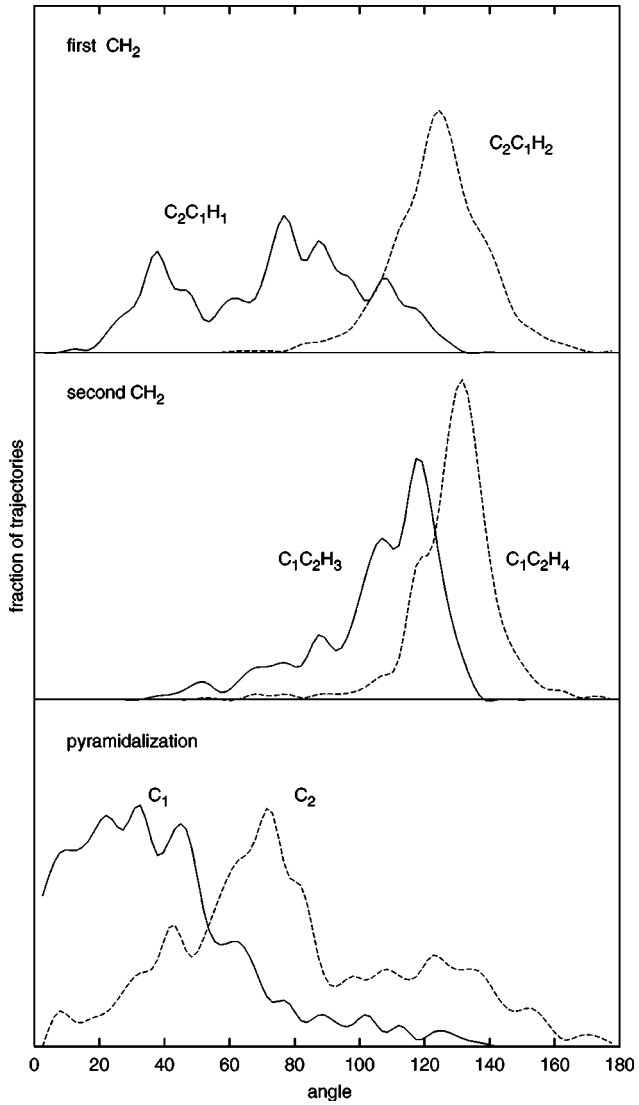

FIG. 3. Distributions of internal coordinates at the time of the first surface hopping. Upper panel, smallest CCH angle ($\angle C_2C_1H_1$) and bond angle for the other hydrogen atom in the same methylene moiety ($\angle C_2C_1H_2$). Middle panel, smaller ($\angle C_1C_2H_3$) and larger ($\angle C_1C_2H_4$) bond angles in the other methylene. Lower panel, smaller (C_1) and larger (C_2) pyramidalization angles.

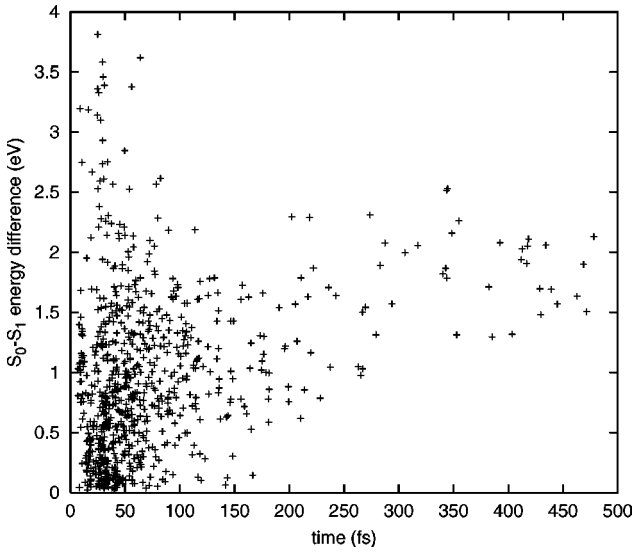

FIG. 4. Distribution of S_0-S_1 energy differences at the time of the first surface hopping.

in AIMS, they concern the calculation of dynamical couplings (the MO derivative terms were neglected in the ethylene calculations), and the truncation of the adaptive basis set, which is dynamically extended only when sufficiently large transition probabilities are envisaged; the latter limitation, which can be gradually relaxed (obviously making the calculation more expensive), may lead to underestimate electronic transitions in regions not close to the crossing seam, and to overestimate the excited state lifetimes. Another and probably more important source of discrepancy are the different PES we used. The semiempirical PES should obviously be improved by reparametrization. The best *ab initio* PES,[17] in comparison with those employed in the AIMS treatment, show a more readily accessible conical intersection, lower in energy and at a smaller pyramidalization angle, which would likely result in a faster decay.

V. CONCLUSIONS

We have described a direct trajectory plus surface-hopping algorithm, using semiempirical MO–CI wave functions, devised to simulate photochemical processes. The molecular orbitals, from which the CI wave functions are built, can be obtained by an SCF procedure with floating occupation numbers, which is able to describe correctly bond breaking processes and orbital (quasi-) degeneracies. The propagation of the time-dependent electronic wave function is done by a norm-conserving algorithm which is inherently stable also in surface crossing situations.

The simple example of ethylene excited state dynamics involves several internal coordinates; the analytical representation of its PES and nonadiabatic couplings would constitute a nontrivial problem, which is very conveniently bypassed in the frame of a direct procedure. Larger systems can be simulated with reasonable computing times: for instance, a short trajectory (<1 ps) of a molecule with 20 atoms requires of the order of an hour on Pentium III processors. The most expensive steps are the semiempirical CPHF and CI calculations,[23] therefore we are currently implementing a QM/MM scheme whereby only a portion of the system is explicitly treated at quantum-mechanical level, and the rest by molecular mechanics.

Our method can be used in conjunction with the standard semiempirical Hamiltonians implemented in the MOPAC package,[21] thus making available a general purpose tool for the simulation of excited state molecular dynamics. Of course its use is subject to caveats, concerning both the semiclassical nature of the dynamical model and the reliability of semiempirical methods. The latter aspect can be taken care of, by ad hoc reoptimization of the semiempirical parameters (see discussion in Sec. II).

In conclusion, we believe this work is a significant step, bringing the simulation of photochemical reactions towards the general applicability and increasing practical usefulness

which already characterize theory and computational methods for thermal reaction rates and mechanisms.

APPENDIX A

The overlap of two CI wave functions at the beginning and at the end of a time step ($t=0$ and $t=\Delta t$) is

$$S_{KL}=\langle\psi_K(0)|\psi_L(\Delta t)\rangle$$

$$=\sum_{IJ} C_{IK}(0)C_{JL}(\Delta t)\langle\Phi_I(0)|\Phi_J(\Delta t)\rangle, \tag{A1}$$

where $\mathbf{C}_K$ and $\mathbf{C}_L$ are CI eigenvectors. The Slater determinants are expressed as

$$\Phi_I(t)=\hat{\mathcal{A}}\left[\prod_i^{N_\alpha}\phi_i(x_i,t)\prod_{i'}^{N_\beta}\overline{\phi}_{i'}(x_{i'},t)\right], \tag{A2}$$

where $\hat{\mathcal{A}}$ is the antisimmetrizer and $\phi_i,\overline{\phi}_{i'}$ are α and β spin–orbitals. The overlap between two determinants is then

$$\langle\Phi_I(0)|\Phi_J(\Delta t)\rangle=(\det\mathbf{A}^{(\mathbf{IJ})})\cdot(\det\mathbf{B}^{(\mathbf{IJ})}), \tag{A3}$$

where $A_{ij}^{(IJ)}=\langle\phi_i(0)|\phi_j(\Delta t)\rangle$ is the overlap between the ith α orbital of Φ_I and the jth of Φ_J; the $\mathbf{B}^{(\mathbf{IJ})}$ matrix is defined in the same way for the β orbitals. The NDO approximation and the diabatization procedures already devised so as to eliminate the electron translation factor[42,43] concur in simplifying the evaluation of the $\langle\phi_i(0)|\phi_j(\Delta t)\rangle$ overlaps, which reduce to scalar products of the orbital coefficient vectors.

If a small active space of N_A orbitals is used, with $N_\alpha+N_\beta$ active α and β electrons, and N_D doubly occupied orbitals, one can speed up the evaluation of $\det\mathbf{A}^{(\mathbf{IJ})}$ and $\det\mathbf{B}^{(\mathbf{IJ})}$, by partitioning the $\mathbf{A}^{(\mathbf{IJ})}$ (and $\mathbf{B}^{(\mathbf{IJ})}$) matrix in blocks of dimension N_D and N_α (or N_β):

$$\mathbf{A}^{(\mathbf{IJ})}=\begin{pmatrix}\mathbf{A}_{\mathbf{DD}} & \mathbf{A}_{\mathbf{D}\alpha}^{(\mathbf{IJ})}\\ \mathbf{A}_{\alpha\mathbf{D}}^{(\mathbf{IJ})} & \mathbf{A}_{\alpha\alpha}^{(\mathbf{IJ})}\end{pmatrix}. \tag{A4}$$

The $\mathbf{A}_{\mathbf{DD}}$ block does not depend on the I,J indexes. We can express each column $(\mathbf{A}_{\mathbf{D}\alpha}^{(\mathbf{IJ})})_j$ of the $\mathbf{A}_{\mathbf{D}\alpha}^{(\mathbf{IJ})}$ matrix as a linear combination of the columns of $\mathbf{A}_{\mathbf{DD}}$, provided $\det\mathbf{A}_{\mathbf{DD}}\neq 0$:

$$(\mathbf{A}_{\mathbf{D}\alpha}^{(\mathbf{IJ})})_j=\sum_{j'} R_{j'j}(\mathbf{A}_{\mathbf{DD}})_{j'}. \tag{A5}$$

The coefficients $R_{j'j}$ can be determined once for all, independently of the indexes I and J, for each ϕ_j orbital belonging to the active space; to this aim, as the $(\mathbf{A}_{\mathbf{DD}})_{j'}$ vectors are not an orthogonal set, we resort to a Gram–Schmidt procedure. If we subtract to each of the last N_α columns of $\mathbf{A}^{(\mathbf{IJ})}$ a linear combination of the first N_D columns, with coefficients $R_{j'j}$, we obtain a new matrix where the $\mathbf{A}_{\mathbf{D}\alpha}^{(\mathbf{IJ})}$ block is zeroed, without changing the determinant. Thus, $\det\mathbf{A}^{(\mathbf{IJ})}=(\det\mathbf{A}_{\mathbf{DD}})\cdot(\det\tilde{\mathbf{A}}_{\alpha\mathbf{D}}^{(\mathbf{IJ})})$, where the columns of $\tilde{\mathbf{A}}_{\alpha\mathbf{D}}^{(\mathbf{IJ})}$ are given by

$$(\tilde{\mathbf{A}}_{\alpha\mathbf{D}}^{(\mathbf{IJ})})_j=(\mathbf{A}_{\alpha\alpha}^{(\mathbf{IJ})})_j-\sum_{j'} R_{j'j}(\mathbf{A}_{\alpha\mathbf{D}}^{(\mathbf{IJ})})_{j'}. \tag{A6}$$

Only the small matrix $\tilde{\mathbf{A}}_{\alpha\mathbf{D}}^{(\mathbf{IJ})}$ and its determinant need to be calculated for each pair I,J.

APPENDIX B

The variation of a diabatic wave function along the trajectory is only due to admixing of electronic states belonging to the external subspace (''intruder states''):

$$\frac{d}{dt}|\eta_I(t)\rangle=\sum_{J>N}|\eta_J(t)\rangle\left\langle\eta_J(t)\left|\frac{d}{dt}\right|\eta_I(t)\right\rangle, \tag{B1}$$

whence

$$|\eta_I(\Delta t)\rangle=|\eta_I(0)\rangle+\sum_{J>N}\int_0^{\Delta t}|\eta_J(t)\rangle\times\left\langle\eta_J(t)\left|\frac{d}{dt}\right|\eta_I(t)\right\rangle dt. \tag{B2}$$

If the coupling between the internal and external subspaces is really negligible, one can approximate $|\eta_I(\Delta t)\rangle\simeq|\eta_I(0)\rangle$; otherwise, it is advisable to expand the internal subspace. With this approximation, from Eq. (15) one gets $\mathbf{T}(\Delta t)\simeq\mathbf{S}$. We observe that one obtains the same result through a linear approximation for the variation of η_I along the trajectory step, i.e.,

$$|\eta_I(t)\rangle\simeq|\eta_I(0)\rangle+\left|\frac{d\eta_I}{dt}\right\rangle_{t=0} t \tag{B3}$$

which implies

$$S_{KL}\simeq T_{KL}(\Delta t)+\sum_I^N\left\langle\eta_K\left|\frac{d\eta_I}{dt}\right\rangle_{t=0} T_{IL}(\Delta t)\Delta t. \tag{B4}$$

The right-hand side reduces to $T_{KL}(\Delta t)$ if the dynamical couplings vanish in the $\{\boldsymbol{\eta}\}$ basis. Thus, while the adiabatic wave functions and energies may undergo nonlinear changes in a time step (state mixing typical of curve-crossing situations), the diabatic ones should behave more smoothly, as expressed by Eq. (B3); however, this ansatz will fail if the state mixing involves the external space.

While $\mathbf{T}$ must be a unitary matrix, $\mathbf{S}$ is only approximately such. Therefore, we resort to a Löwdin orthogonalization of the columns of $\mathbf{S}$,

$$\mathbf{T}(\Delta t)=\mathbf{S}\mathbf{O}\boldsymbol{\Lambda}^{-1/2}\mathbf{O}^t, \tag{B5}$$

where $\boldsymbol{\Lambda}$ is the diagonal matrix of the eigenvalues of $\mathbf{S}^t\mathbf{S}$ and $\mathbf{O}$ the diagonalizing transformation

$$\mathbf{S}^t\mathbf{S}\mathbf{O}=\mathbf{O}\boldsymbol{\Lambda}. \tag{B6}$$

From $\mathbf{T}(\Delta t)$ and the adiabatic energies $\mathbf{E}(\Delta t)$ one gets the diabatic Hamiltonian at the end of the time step:

$$\mathbf{H}(\Delta t)=\mathbf{T}(\Delta t)\mathbf{E}(\Delta t)\mathbf{T}^t(\Delta t). \tag{B7}$$

The $\mathbf{H}$ matrix lends itself to a linear interpolation, because it is built on the almost invariant basis $\{\boldsymbol{\eta}\}$; therefore we can write

$$\mathbf{H}(t)\simeq\mathbf{E}(0)+[\mathbf{H}(\Delta t)-\mathbf{E}(0)]\frac{t}{\Delta t}. \tag{B8}$$

With this approximation, Eq. (14) is easily integrated to yield

$$\mathbf{D}(\Delta t)=e^{-i\int_0^{\Delta t}\mathbf{H}(t)dt}\mathbf{D}(0)=e^{-i\mathbf{Z}\Delta t}\mathbf{D}(0), \tag{B9}$$

where $\mathbf{Z}=[\mathbf{E}(0)+\mathbf{H}(\Delta t)]/2$. The exponentiation of the symmetric matrix $\mathbf{Z}$ requires its diagonalization:

$$\mathbf{Z}\mathbf{X}_K=\zeta_K\mathbf{X}_K, \tag{B10}$$

$$e^{-i\mathbf{Z}\Delta t}=\sum_K^N \mathbf{X}_K e^{-i\zeta_K\Delta t}\mathbf{X}_K^t. \tag{B11}$$

The approximate equalities we rely upon, (B3) and (B8), imply errors of the order of Δt^2. Analogous equations involving adiabatic quantities would be useless in surface crossing situations with interaction regions of very narrow span, of the order of $\dot{Q}\Delta t$.

ACKNOWLEDGMENTS

This work has been financially supported by the Italian MURST, through the project ''Theoretical models and computational methods of the structure, dynamic and spectroscopic properties of molecules and clusters.''

[1] M. Persico, I. Cacelli, and A. Ferretti, J. Chem. Phys. **94**, 5508 (1991).
[2] M. Oppel and G. K. Paramonov, Chem. Phys. Lett. **313**, 332 (1999).
[3] A. Toniolo and M. Persico, J. Comput. Chem. **22**, 968 (2001).
[4] S. Clifford, M. J. Bearpark, F. Bernardi, M. Olivucci, M. A. Robb, and B. R. Smith, J. Am. Chem. Soc. **242**, 27 (1995).
[5] W. Domcke and G. Stock, Adv. Chem. Phys. **100**, 1 (1997).
[6] H. Köppel and W. Domcke, ''Vibronic dynamics of polyatomic molecules,'' in *Encyclopedia of Computational Chemistry*, edited by P. v. R., Schleyer, N. L. Allinger, T. Clark, J. Gasteiger, P. A. Kollman, H. F. Schaefer III, and P. R. Schreiner (Wiley, Chichester, 1998).
[7] G. H. Peslherbe, B. M. Ladanyi, and J. T. Hynes, J. Phys. Chem. A **102**, 4100 (1998).
[8] P. Cattaneo, M. Persico, and A. Tani, Chem. Phys. **246**, 315 (1999).
[9] M. D. Hack, A. W. Jasper, Y. L. Volobuev, D. W. Schwenke, and D. G. Truhlar, J. Phys. Chem. A **104**, 217 (2000).
[10] T. Pacher, L. S. Cederbaum, and H. Köppel, Adv. Chem. Phys. **84**, 293 (1993).
[11] M. Persico, ''Electronic diabatic states: Definition, computation and applications,'' in *Encyclopedia of Computational Chemistry*, edited by P. v. R. Schleyer, N. L. Allinger, T. Clark, J. Gasteiger, P. A. Kollman, H. F. Schaefer III, and P. R. Schreiner (Wiley, Chichester, 1998), p. 852.
[12] A. Warshel and R. M. Weiss, J. Am. Chem. Soc. **102**, 6218 (1980).
[13] J. Åqvist and A. Warshel, Chem. Rev. **93**, 2523 (1993).
[14] C. Leforestier, J. Chem. Phys. **68**, 4406 (1978).
[15] R. Car and M. Parrinello, Phys. Rev. Lett. **55**, 2471 (1985).
[16] T. Vreven, F. Bernardi, M. Garavelli, M. Olivucci, M. A. Robb, and H. B. Schlegel, J. Am. Chem. Soc. **119**, 12687 (1997).
[17] M. Ben-Nun, J. Quenneville, and T. J. Martinez, J. Phys. Chem. A **104**, 5161 (2000).
[18] A. L. Kaledin and K. Morokuma, J. Chem. Phys. **113**, 5750 (2000).
[19] J. E. Ridly and M. C. Zerner, Theor. Chim. Acta **42**, 223 (1976).
[20] I. Baraldi, A. Carnevali, F. Momicchioli, and G. Ponterini, Spectrochim. Acta, Part A **49A**, 471 (1993).
[21] J. J. P. Stewart, MOPAC 2000, Fujitsu Limited, Tokyo, Japan, 1999.
[22] A. Germain and P. Millié, Chem. Phys. **219**, 265 (1997).
[23] G. Granucci and A. Toniolo, Chem. Phys. Lett. **325**, 79 (2000).
[24] J. C. Tully, J. Chem. Phys. **93**, 1061 (1990).
[25] J. C. Tully, Int. J. Quantum Chem., Symp. **25**, 299 (1991).
[26] A. Ferretti, G. Granucci, A. Lami, M. Persico, and G. Villani, J. Chem. Phys. **104**, 5517 (1996).
[27] P. Cattaneo and M. Persico, J. Phys. Chem. A **101**, 3454 (1997).
[28] Y. L. Volobuev, M. D. Hack, and D. G. Truhlar, J. Phys. Chem. A **103**, 6225 (1999).
[29] F. Santoro, C. Petrongolo, G. Granucci, and M. Persico, Chem. Phys. **259**, 193 (2000).
[30] J. Slater, J. B. Mann, T. M. Wilson, and J. H. Wood, Phys. Rev. **194**, 672 (1969).
[31] H. F. King and R. E. Stanton, J. Chem. Phys. **50**, 3789 (1969).
[32] A. R. Rabuck and G. E. Scuseria, J. Chem. Phys. **110**, 695 (1999).
[33] W. H. Press, S. A. Teukolsky, W. T. Vetterling, and B. P. Flannery, *Numerical Recipes in Fortran 77* (Cambridge University Press, Cambridge, 1992).
[34] R. C. Bingham, M. J. S. Dewar, and D. H. Lo, J. Am. Chem. Soc. **97**, 1285 (1975).
[35] M. J. S. Dewar, E. G. Zoebisch, E. F. Healy, and J. J. P. Stewart, J. Am. Chem. Soc. **107**, 3902 (1985).
[36] W. Thiel and A. Voityuk, J. Phys. Chem. **100**, 616 (1996).
[37] S. Inglese, thesis, University of Pisa, 2000.
[38] L. Verlet, Phys. Rev. **159**, 98 (1967).
[39] W. F. van Gunsteren and H. J. C. Berendsen, Mol. Phys. **45**, 637 (1982).
[40] P. Cattaneo, G. Granucci, and M. Persico, J. Phys. Chem. A **103**, 3364 (1999).
[41] M. Baer, Chem. Phys. **15**, 49 (1976).
[42] F. X. Gadéa and M. Pélissier, J. Chem. Phys. **93**, 545 (1990).
[43] I. D. Petsalakis, G. Teodorakopoulos, and C. A. Nicolaides, J. Chem. Phys. **97**, 7623 (1992).
[44] J.-Y. Fang and S. Hammes-Schiffer, J. Phys. Chem. A **103**, 9399 (1999).
[45] R. M. Weiss and A. Warshel, J. Am. Chem. Soc. **101**, 6131 (1979).
[46] M. Persico, J. Am. Chem. Soc. **102**, 7839 (1980).
[47] M. Ben-Nun and T. J. Martinez, Chem. Phys. Lett. **298**, 57 (1998).
[48] P. Farmanara, V. Stert, and W. Radloff, Chem. Phys. Lett. **288**, 518 (1998).
[49] J. M. Mestdagh, J. P. Visticot, M. Elhanine, and B. Soep, J. Chem. Phys. **113**, 237 (2000).
[50] I. Ohmine, J. Chem. Phys. **83**, 2348 (1985).
[51] A. M. Mebel, Y.-T. Chen, and S.-H. Lin, J. Chem. Phys. **105**, 9007 (1996).
[52] At planar geometries the lowest excited state is of Rydberg character, a feature which cannot be correctly reproduced in a standard semiempirical framework, or even by *ab initio* calculations without the use of diffuse basis functions. However, already at moderate torsion angles, the Rydberg character disappears, so it should not influence the relaxation dynamics in an important way.